Developmental Cell
Article

Patched1 Haploinsufficiency Increases Adult Bone Mass and Modulates Gli3 Repressor Activity

Shinsuke Ohba,[1,2,8,*] Hiroshi Kawaguchi,[1] Fumitaka Kugimiya,[1] Toru Ogasawara,[1] Naohiro Kawamura,[1] Taku Saito,[1] Toshiyuki Ikeda,[1] Katsunori Fujii,[3] Tsuyoshi Miyajima,[4] Akira Kuramochi,[5] Toshiyuki Miyashita,[6] Hiromi Oda,[4] Kozo Nakamura,[1] Tsuyoshi Takato,[1] and Ung-il Chung[2,7,*]
[1]Department of Sensory and Motor System Medicine
[2]Center for Disease Biology and Integrative Medicine
Graduate School of Medicine, The University of Tokyo, Bunkyo-ku, Tokyo 113-8655, Japan
[3]Department of Pediatrics, Graduate School of Medicine, Chiba University, Chiba-shi, Chiba 260-8670, Japan
[4]Department of Orthopedic Surgery
[5]Department of Dermatology
Saitama Medical School, Iruma-gun, Saitama 350-0495, Japan
[6]Department of Genetics, National Research Institute for Child Health and Development, Setagaya-ku, Tokyo 157-8535, Japan
[7]Department of Bioengineering, Graduate School of Engineering, The University of Tokyo, Bunkyo-ku, Tokyo 113-8655, Japan
[8]Department of Molecular and Cellular Biology, Harvard University, Cambridge, MA 02138, USA
*Correspondence: shin-o@umin.ac.jp (S.O.), uichung-tky@umin.ac.jp (U.-i.C.)
DOI 10.1016/j.devcel.2008.03.007

SUMMARY

Hedgehog (Hh)-Patched1 (Ptch1) signaling plays essential roles in various developmental processes, but little is known about its role in postnatal homeostasis. Here, we demonstrate regulation of postnatal bone homeostasis by Hh-Ptch1 signaling. *Ptch1*-deficient (*Ptch1*$^{+/-}$) mice and patients with nevoid basal cell carcinoma syndrome showed high bone mass in adults. In culture, *Ptch1*$^{+/-}$ cells showed accelerated osteoblast differentiation, enhanced responsiveness to the runt-related transcription factor 2 (Runx2), and reduced generation of the repressor form of Gli3 (Gli3rep). Gli3rep inhibited DNA binding by Runx2 in vitro, suggesting a mechanism that could contribute to the bone phenotypes seen in the *Ptch1* heterozygotes. Moreover, systemic administration of the Hh signaling inhibitor cyclopamine decreased bone mass in adult mice. These data provide evidence that Hh-Ptch1 signaling plays a crucial role in postnatal bone homeostasis and point to Hh-Ptch1 signaling as a potential molecular target for the treatment of osteoporosis.

INTRODUCTION

Hh-Ptch1 signaling is a highly conserved pathway, and its activities are central to the patterning and morphogenesis of many different regions within the bodies of vertebrates and insects (Ingham and McMahon, 2001). In the conventional model of Hh signal transduction, Smoothened (Smo), a seven-pass transmembrane protein, has an intrinsic intracellular signaling activity that is repressed by Patched (Ptch). Ptch is a 12-pass transmembrane receptor of Hh, and two *Ptch* genes, *Ptch1* and *Ptch2*, have been identified in vertebrates. The binding of Hh ligands to Ptch relieves Ptch's repressive effect on Smo, initiating Hh-Ptch1 signal transduction. In vertebrates, intracellular signaling activity is mediated through the zinc finger transcription factors Gli1, Gli2, and Gli3 (Ingham and McMahon, 2001). Hh-Ptch1 signaling suppresses the processing of Gli2 and Gli3 into transcriptional repressor forms. Gli2 is suggested to function primarily as a transcriptional activator, and Gli3 as a transcriptional repressor, although some studies have shown the opposite (Ingham and McMahon, 2001). On the other hand, Gli1 is one of the transcriptional targets of Hh-Ptch1 signaling and functions as a strong transcriptional activator (Ingham and McMahon, 2001). Hh-Ptch1 signaling exerts its diverse and potent activities through such complicated regulations of Gli proteins.

We and others have clarified the essential roles of Hh-Ptch1 signaling in bone development through analyses of *Ihh*-deficient mice (*Ihh*$^{-/-}$) (St-Jacques et al., 1999), *Ihh*$^{-/-}$/wild-type (WT) chimeric mice (Chung et al., 2001), and *Smo*-deficient (*Smo*$^{-/-}$)/WT chimeric mice (Long et al., 2004). These results revealed that local production of Ihh by hypertrophic chondrocytes and direct input of Ihh to osteoblast precursors are required for bone formation. *Gli1* is not essential for initial Hh signal transduction and is dispensable for mouse development (Park et al., 2000), but loss of *Gli2* or *Gli3* in mice results in severe skeletal and neural defects and embryonic or perinatal lethality (Hui and Joyner, 1993; Mo et al., 1997). Removal of *Gli3* in *Shh*$^{-/-}$ mice rescues a multitude of defects in limb patterning (Litingtung et al., 2002), and removal of *Gli3* in *Ihh*$^{-/-}$ mice partially rescues defects in osteoblast development (Hilton et al., 2005). Furthermore, Hh-regulated processing of Gli3 has an important role in developing limbs (Wang et al., 2000). These lines of evidence suggest that Gli3 is a critical mediator of Hh activity, especially in skeletal development. This idea is further supported by analysis of Greig cephalopolysyndactyly syndrome (GCPS) and Pallister-Hall syndrome (PHS), two autosomal dominant syndromes associated with different types of mutations in the *GLI3* locus. Although GCPS and PHS are distinct clinical entities with numerous nonoverlapping features, both syndromes manifest similar skeletal abnormalities including preaxial polydactyly (Johnston et al., 2005). Furthermore, nevoid basal cell carcinoma syndrome

(NBCCS or Gorlin syndrome), another autosomal dominant syndrome associated with *PTCH1* haploinsufficiency, is also characterized by skeletal abnormalities partly similar to those of GCPS and PHS (Gorlin, 1987). These lines of evidence suggest that the repressive effect of *PTCH1* and *GLI3* on Hh-Ptch1 signaling has a crucial role in the skeletal system.

Ptch1 has emerged as a tumor suppressor gene and developmental regulator. Homozygous *Ptch1*-deficient ($Ptch1^{-/-}$) mice die at around day 9.5 of embryogenesis with neural tube defects, and derepression of Hh target genes occurs as a consequence of ectopic activation of Smo (Goodrich et al., 1997). Heterozygous *Ptch1*-deficient ($Ptch1^{+/-}$) mice have features that partly recapitulate those of NBCCS (Goodrich et al., 1997). The patients are characterized by skeletal abnormalities, craniofacial abnormalities, large body size, and tumors, including basal cell carcinomas of the skin and cerebellar medulloblastomas (Gorlin, 1987). Studies of $Ptch1^{+/-}$ mice have established the roles of Hh-Ptch1 signaling in tumorigenesis (Goodrich et al., 1997; Wetmore et al., 2000), body size determination, and limb patterning (Goodrich et al., 1997; Milenkovic et al., 1999). Despite these extensive studies, little is known about the involvement of *Ptch1* in bone formation and postnatal bone homeostasis. It also remains unclear which transcriptional factors are involved in the control of osteoblast differentiation downstream of Hh-Ptch1 signaling.

This study aimed to determine the physiological function of Hh-Ptch1 signaling in postnatal bone homeostasis, and to clarify the underlying molecular mechanisms, focusing particularly on transcriptional regulation of osteogenesis-related genes.

RESULTS

Ptch1 Haploinsufficiency Increases Bone Mass In Vivo

$Ptch1^{-/-}$ mice died between embryonic days (E) 9.0 and 10.5 (Goodrich et al., 1997); so to investigate the physiological role of *Ptch1* in bone metabolism, we analyzed the skeletal system in $Ptch1^{+/-}$ mice at 8 weeks of age. $Ptch1^{+/-}$ mice grew without gross skeletal abnormalities, and X-ray and 3D-CT analyses of femurs and tibias revealed that $Ptch1^{+/-}$ mice had increased bone mass compared to the wild-type littermates (WT) (Figure 1A). The bone mineral density (BMD) of these bones was significantly increased in $Ptch1^{+/-}$ mice (Figure 1B). von Kossa staining and calcein double labeling of the tibias revealed an increase in trabecular bone mass due to accelerated bone formation in $Ptch1^{+/-}$ mice, whereas toluidine blue staining revealed no obvious abnormalities in the epiphyseal plates (Figure 1C). Bone histomorphometric analyses revealed that parameters for bone formation were markedly increased in $Ptch1^{+/-}$ mice (Figure 1D), suggesting that *Ptch1* haploinsufficiency enhances osteoblast differentiation and matrix synthesis. $Ptch1^{+/-}$ mice also had greater numbers of tartrate-resistant acid phosphatase (TRAP)-positive osteoclasts (Figure 1E), and all parameters of bone resorption were significantly increased in $Ptch1^{+/-}$ mice (Figure 1F). Accelerated osteogenesis was also observed in E17.5 $Ptch1^{+/-}$ embryos without gross abnormalities in skeletal patterning or differentiation of growth plate chondrocytes (Figures S1A–S1C; see the Supplemental Data available with this article online). These results suggest that *Ptch1* haploinsufficiency causes high bone mass in adult mice due to an increase in bone formation, and this phenotype starts at the fetal stage.

The phenotype of $Ptch1^{+/-}$ mice, a model for NBCCS, led us to ask whether or not bone mass was affected in NBCCS patients. We had the opportunity to measure BMDs of the lumbar spine and femoral neck in two patients (one male, one female). They had been diagnosed as having NBCCS based on diagnostic criteria (Gorlin, 1987) or on the identification of mutations in the *PTCH1* gene (Fujii et al., 2003a, 2003b). When compared to age- and gender-matched controls, the patients had high BMDs (Table S1). The serum level of bone-specific ALP and the urine level of deoxypyridinolines of the male patient were markedly elevated (Table S1), suggesting increased bone metabolism. This finding in NBCCS patients is consistent with the phenotypes observed in $Ptch1^{+/-}$ mice.

Ptch1 Haploinsufficiency Enhances Osteoblast Differentiation In Vitro

To identify which cells contribute to the skeletal phenotype of $Ptch1^{+/-}$ mice, we performed ex vivo cultures of primary bone cells from WT and $Ptch1^{+/-}$ mice. There was no significant difference in cell proliferation of bone marrow stromal cells (BMSCs) and osteoblast precursors (OPs) between $Ptch1^{+/-}$ and WT (Figure S2). However, osteoblast differentiation was accelerated by *Ptch1* haploinsufficiency in both cell types, as indicated by the enhancement of alkaline phosphatase (ALP) activity and calcified nodule formation (Figures 2A and 2B) and by upregulation of osteoblast marker gene expression (Figures 2C and 2D).

Endogenous BMPs have crucial roles in bone formation (Hoffmann and Gross, 2001), and Runx2 is essential for both endochondral and intramembranous bone development (Ducy et al., 1997; Komori et al., 1997). In addition, we and others reported that BMP signaling and Runx2 synergistically work as potent inducers of osteoblast differentiation (Bae et al., 2007; Ohba et al., 2007; Phimphilai et al., 2006; Yang et al., 2003). Furthermore, two recent studies highlighted novel mechanisms underlying the Hh/Gli2- and Hh/Gli3-mediated osteoblast differentiation, focusing on regulation of BMP2 expression (Zhao et al., 2006; Garrett et al., 2003), induction of Runx2 expression, and regulation of Runx2 function (Shimoyama et al., 2007). In light of these reports, to gain insight into mechanisms underlying accelerated osteoblast differentiation in $Ptch1^{+/-}$, we investigated the expression of Runx2 and Bmp2, 4, 6, and 7. As shown in Figures 2E–2G, there were no obvious differences in the mRNA expression of *Runx2*, the protein expression of Runx2, or the mRNA expression of *Bmps* between $Ptch1^{+/-}$ and WT cells. However, the response to exogenously introduced Runx2 and to recombinant human BMP2 (rhBMP2) was markedly enhanced in $Ptch1^{+/-}$ cells (Figure 2H). These data suggest that *Ptch1* haploinsufficiency enhances osteoblast differentiation by augmenting Runx2 and/or BMP/Smad signaling, but not by inducing the expression of Runx2 and Bmps.

We also examined the role of *Ptch1* in osteoclast differentiation and found that osteoclast precursors including primary bone marrow macrophages (BMMϕ) and RAW264.7 cells expressed *Ptch1* mRNA (Figure S3A). Coculture of calvarial OPs and BMMϕ showed that osteoclastogenesis was enhanced when OPs, but not BMMϕ, were derived from $Ptch1^{+/-}$ mice

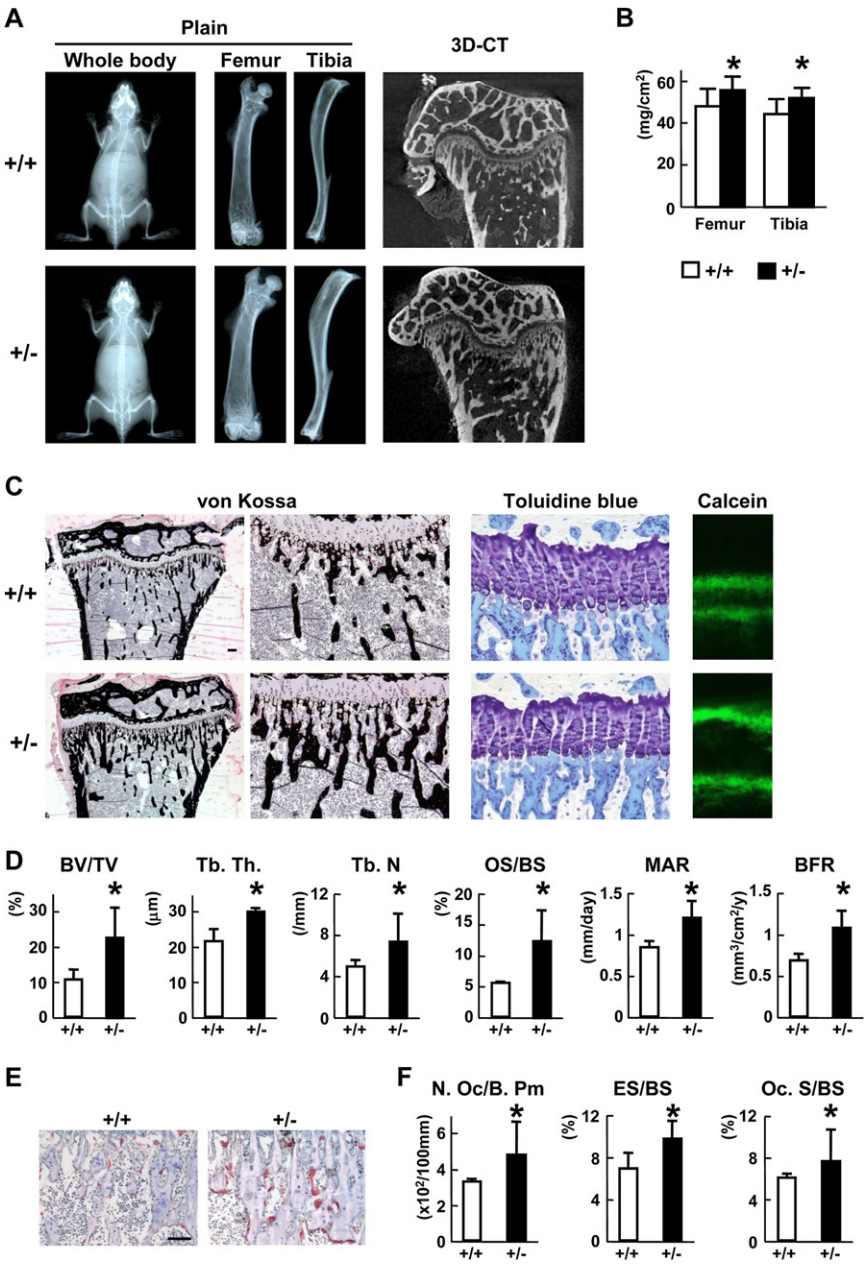

Figure 1. Radiological and Histological Analyses of Adult WT and *Ptch1*$^{+/-}$ Littermates

(A) Plain X-ray images of the whole bodies, femurs and tibias, and three-dimensional CT images of the medial tibias of representative 8-week-old WT and *Ptch1*$^{+/-}$ mice.

(B) Bone mineral density of the whole femurs and tibias from 8-week-old WT and *Ptch1*$^{+/-}$ mice. Data are means ± SDs of ten mice per genotype. *$p < 0.05$ versus WT.

(C) von Kossa staining, toluidine blue staining, and calcein double labeling of the proximal tibia sections of representative 8-week-old WT and *Ptch1*$^{+/-}$ mice. Bar, 300 μm.

(D) Histomorphometric analyses of bone volume and bone formation parameters in the proximal tibias of 8-week-old WT and *Ptch1*$^{+/-}$ mice. BV/TV, trabecular bone volume per tissue volume; Tb. Th, trabecular thickness; Tb. N., trabecular number; OS/BS, osteoid surface per bone surface; MAR, mineral apposition rate; BFR bone formation rate per bone surface.

(E) TRAP staining of the proximal tibia sections of representative 8-week-old WT and *Ptch1*$^{+/-}$ mice. Bar, 300 μm.

(F) Histomorphometric analyses of bone resorption parameters in the proximal tibia. N. Oc/B. Pm, number of osteoclasts per 100 mm of bone perimeter; ES/BS, eroded surface per bone surface; Oc. S/BS, osteoclast surface per bone surface. For (D) and (F), data are means ± SDs of five mice per genotype. *$p < 0.05$ versus WT.

(Figure S3B). Furthermore, expression of the receptor activator of nuclear factor-κB ligand (*Rankl*) was markedly upregulated in *Ptch1*$^{+/-}$ OPs, whereas that of osteoprotegerin was not (Figure S3C). These results suggest that the enhanced bone resorption in *Ptch1*$^{+/-}$ mice was a secondary effect of increased osteoblast activity, and that upregulation of *Rankl* was at least partly responsible for mediating the effect.

Ptch1 Haploinsufficiency Causes Activation of Hh Signaling and Alters Expression of Gli3 in Osteoblast Precursors

To explore downstream mediators of *Ptch1* haploinsufficiency, we examined the effect of *Ptch1* haploinsufficiency on Hh-Ptch1 signaling in cultured OPs. Expression of *Ptch1* mRNA was reduced in *Ptch1*$^{+/-}$ cells (Figure 3A). *Gli1* mRNA, a readout of Hh-Ptch1 signaling, was upregulated in *Ptch1*$^{+/-}$ OPs (Figure 3A), suggesting that *Ptch1* haploinsufficiency led to constitutive activation of Hh signaling. Hh signaling has been demonstrated to suppress *Gli3* transcription and processing in mouse limb bud cells (Wang et al., 2000) as well as Gli2 processing and degradation in mouse embryonic fibroblasts (Pan et al., 2006). Based on these reports, we investigated the expression patterns of Gli2 and Gli3 in *Ptch1*$^{+/-}$ and WT OPs. Expression of *Gli3* mRNA (Figure 3A), that of Gli3 proteins, and the processing of the full-length forms of Gli3 (Gli3-190, Gli3full) into the repressor form of Gli3 (Gli-83, Gli3rep) were markedly reduced in *Ptch1*$^{+/-}$ OPs (Figure 3B). Furthermore, Gli3rep, but not Gli3full, preferentially accumulated in the nucleus and colocalized with Runx2 (Figure 3C), which itself was not altered by *Ptch1* haploinsufficiency (data not shown). By contrast, mRNA expression of *Gli2* was not noticeably altered, and no alteration in Gli2 expression, processing, or localization was detected (Figure 3A and Figure S4). These results suggest that *Ptch1* haploinsufficiency causes constitutive activation of Hh signaling and represses the generation of Gli3rep, which may interact with osteogenesis-related transcription factors such as Runx2 in the nucleus.

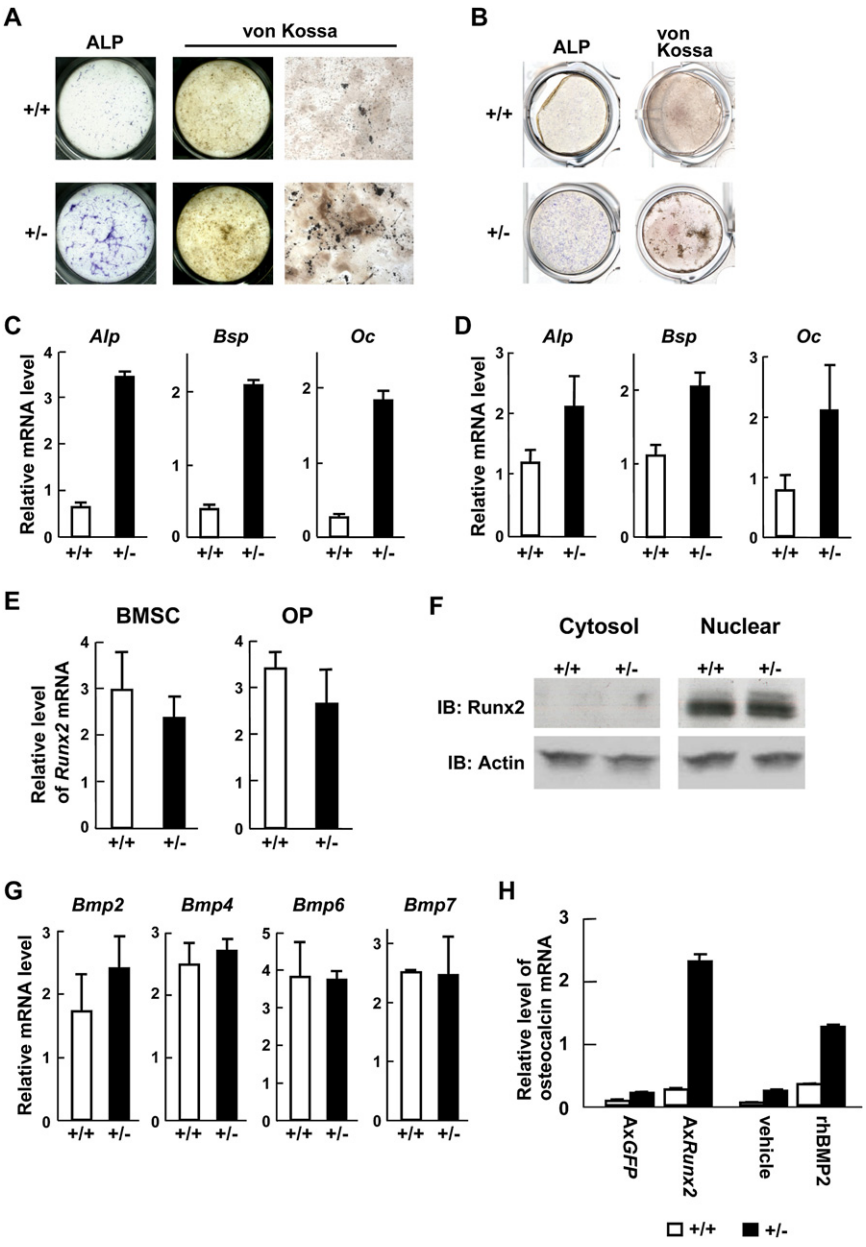

Figure 2. Osteoblast Differentiation in Cultures of Precursor Cells from WT and *Ptch1*$^{+/-}$ Littermates

(A and B) ALP and von Kossa staining in osteogenic cultures of BMSCs (A) and OPs (B). For ALP staining, cells were cultured for 10 days. For von Kossa staining, cells were cultured for 20 days. Representative pictures of independent experiments are shown.

(C and D) mRNA expression of osteoblast marker genes in 20-day osteogenic cultures of BMSCs (C) and OPs (D). mRNA expression was analyzed by real-time RT-PCR analysis. *Alp*, alkaline phosphatase; *Bsp*, bone sialoprotein; *Oc*, osteocalcin.

(E) *Runx2* mRNA expression determined by real-time RT-PCR analysis in 20-day osteogenic cultures of BMSCs and OPs.

(F) Protein expression of endogenous Runx2 in OPs cultured for 20 days. Protein expression was analyzed by immunoblot analysis using specific antibodies. IB, immunoblot.

(G) mRNA expression of *Bmps* determined by real-time RT-PCR analysis in 20-day osteogenic cultures of OPs.

(H) *Osteocalcin* mRNA expression determined by real-time RT-PCR analysis in osteogenic culture of BMSCs. Cells were infected with adenoviruses expressing GFP or Runx2; or treated with or without recombinant human BMP2 and cultured for 7 days. For (C)–(E), (G), and (H), data are means ± SDs of triplicate wells, and representative data of independent experiments are shown.

Gli3rep Attenuates Runx2 Transcriptional Activity by Competitively Inhibiting DNA Binding of Runx2

The data so far suggest that Gli3 acts as a key downstream mediator of Hh-Ptch1 signaling-induced osteoblast differentiation. To test this hypothesis, we investigated the effect of loss or overexpression of *Gli3* on osteoblast differentiation. Hh signaling-induced osteoblast differentiation was compared between *Gli3*$^{Xt\text{-}J/Xt\text{-}J}$ (*Gli3*$^{-/-}$) and WT calvarial cells (Hui and Joyner, 1993). ALP activity and calcification of WT cells were enhanced upon treatment with a Hh agonist (Hh-ago) (Figure 4A). In *Gli3*$^{-/-}$ cells, ALP activity and calcification were remarkably enhanced without Hh-ago treatment, and the treatment with Hh-ago had little further effect (Figure 4A). In contrast, overexpression of *Gli3rep*, but not that of *Gli3full*, decreased osteocalcin expression in WT cells (Figure 4B). These data support the above hypothesis.

They also suggest that Gli3 functions as a potent repressor of osteoblast differentiation and that, of the two different forms, Gli3rep plays a central role. Furthermore, Gli3rep downregulated Runx2-dependent expression of osteocalcin in C3H10T1/2 cells without affecting protein levels of Runx2 (Figure 4B and Figure S5). In addition, the loss or overexpression of *Gli3rep* in osteoblasts did not affect protein expression of osteogenesis-related transcription factors and cofactors including Smad1, Smad2/3, Osterix, LEF, β-catenin, Runx2, and Cbfb (Figure S6). These results raised the possibility that Gli3rep had a negative impact on osteoblast differentiation by posttranslationally interfering with the function of osteogenesis-related transcription factors.

To test this hypothesis, we examined the effect of Gli3rep on the transcriptional activities of Runx2, β-catenin-LEF1, Smad1, Smad3, and Osterix using luciferase reporter plasmids driven by the osteocalcin promoter (1050 Oc), LEF-binding site (Topflash), Smad1-responsive elements (12×GCCG), Smad3-responsive elements (9×CAGA), and type I collagen promoter (2.3 kb Col1a1), respectively. Gli3rep repressed the transcriptional activities of Runx2 and β-catenin-LEF1 complex and enhanced that of Smad3. On the other hand, Gli3rep did not alter the transcriptional activities of Smad1 or Osterix (Figure 4C). Among Runx2, LEF1, and Smad3, we focused on characterizing

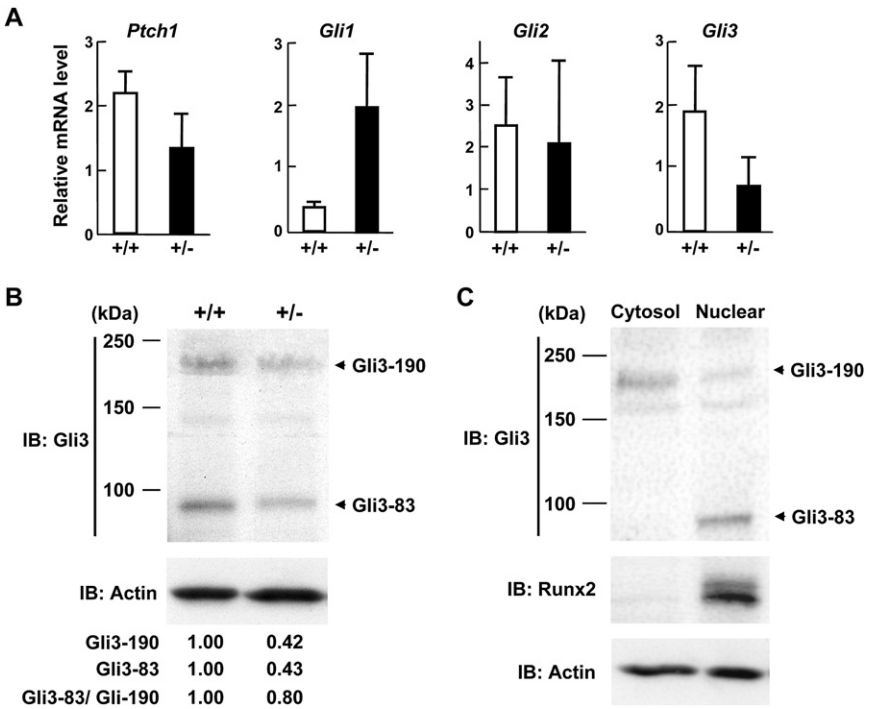

Figure 3. Constitutive Activation of Hh-Ptch1 Signaling and Alteration of Gli3 Processing in OPs from WT and *Ptch1*$^{+/-}$ Littermates

(A) mRNA expression of Hh-Ptch1 signaling mediators in OPs cultured for 10 days in α-MEM/10% FBS, determined by real-time RT-PCR analysis. Data are means ± SDs of triplicate wells, and representative data of independent experiments are shown.

(B) Protein expression of endogenous Gli3 in OPs cultured for 10 days in α-MEM/10% FBS. Expression was analyzed by immunoblot analysis using specific antibodies. Quantification of their band intensities was performed by normalization to those of actin in each group, and the data are shown below the pictures. Gli-83/Gli-190, relative band intensity of Gli-83 to Gli-190 in each group.

(C) Localization of endogenous Gli3 and Runx2 in WT OPs cultured for 10 days in α-MEM/10% FBS. IB, immunoblot; Cytosol, cytosol fraction; Nuclear, nuclear fraction. For (B) and (C), the positions of full-length (Gli-190) and processed (Gli-83) Gli3 proteins are denoted by arrows.

the interaction between Runx2 and Gli3rep, because the inhibitory action of Gli3rep on Wnt-mediated transcription (Ulloa et al., 2007) and the interaction between Gli3rep and Smad3 (Liu et al., 1998) have already been reported. The repressive effect of Gli3rep on Runx2-dependent transcription is not affected by the presence or absence of Cbfb, the most potent cofactor of Runx2 (Figure 4C), suggesting that Gli3rep exerts its effect through Runx2 but not through Cbfb. We next performed luciferase assays using a series of deletion constructs of the osteocalcin promoter (−962, −647, −442, −230, 6×OSE2) to identify regions responsible for the transcriptional inhibition by Gli3rep. In all constructs, Gli3rep repressed the Runx2-dependent transcriptional activity, suggesting that the response region for Gli3rep was located within the OSE2 site (Figure 4D). Computer analysis of the OSE2 sequence identified a putative Gli-binding site (Gli-BS), which partly overlapped with the Runx2-binding site. Mutations of the Gli-BS in OSE2 diminished the repression by Gli3rep (Figure 4E), suggesting that the Gli-BS in OSE2 is responsible for Gli3rep's repressive effect on Runx2-dependent transcription.

To investigate the specificity of repression of Runx2-dependent transcription by Gli3rep, we compared the repressive effects of Gli1, Gli2, Gli3full, and Gli3rep. In a luciferase assay using 6×OSE2, only Gli3rep, and not the other Glis, had a repressive effect on Runx2-dependent transcription (Figure 5A). The functions of the Gli vectors used here were verified by their effects on 8×Gli-BS Luc as previously reported (Sasaki et al., 1999) (Figure 5A). EMSA using nuclear extracts of *Glis*-transfected cells revealed that only Gli3rep could bind to OSE2 (Figure 5B, lanes 1–16). The DNA-binding activity of Runx2 was attenuated in cells transfected with *Runx2* and *Gli3rep*, as compared to *Runx2*-transfected cells (Figure 5B, lanes 9 and 13–16). At the same time, Gli3rep's binding activity to Gli-BS in the *Ptch1* promoter sequence was maintained (Figure 5B, lanes 20–25), suggesting that the experimental conditions did not affect the original function of Gli3rep. Competition binding assays using unlabeled-WT or -mutated probes showed that Runx2 and Gli3rep bound to their binding sites within OSE2, which partly overlapped (Figure 5B, lanes 13 and 17–19). Furthermore, when the nuclear extract of *Gli3rep*-transfected cells was added to the binding mixture containing the extract of *Runx2*-transfected ones, DNA binding of Runx2 was inhibited in a dose-dependent manner, with increasing DNA binding of Gli3rep (Figure 5C). Similarly, the addition of the recombinant Gli3rep protein to the binding mixture caused inhibition of DNA binding of Runx2 in a dose-dependent manner, and the addition of anti-Gli3 antibody attenuated the inhibition by Gli3rep (Figure S7). On the other hand, Gli3rep did not affect DNA binding by the LEF1-β-catenin complex or the Smad3-Smad4 complex (Figure S8), although it did alter their transcriptional activities (Figure 4C), arguing against the possibility that the inhibitory effect of Gli3rep on DNA binding of Runx2 was nonspecific. To explore this inhibitory effect further in a genomic DNA context, we performed chromatin immunoprecipitation (ChIP) of extracts isolated from C3H10T1/2 cells transfected with *Runx2*, *Gli3rep*, or both. As shown in Figure 5D, recruitment of Gli3rep onto OSE2 in the osteocalcin promoter was readily detected, and that of Runx2 was decreased by cotransfection of *Gli3rep*. In addition, a physical association between Runx2 and Gli3rep was not discernible in our experiments (data not shown). Finally, we examined the DNA binding activity of Runx2 in *Gli3*$^{-/-}$ and *Ptch1*$^{+/-}$ OPs by EMSA. The activity was augmented in both mutants as compared to WT littermates (Figure 5E), supporting our findings so far about the overexpression of Gli3rep. These lines of evidence suggest that Gli3rep attenuates Runx2 transcriptional activity by competitively inhibiting DNA binding of Runx2 to OSE2, and that excessive

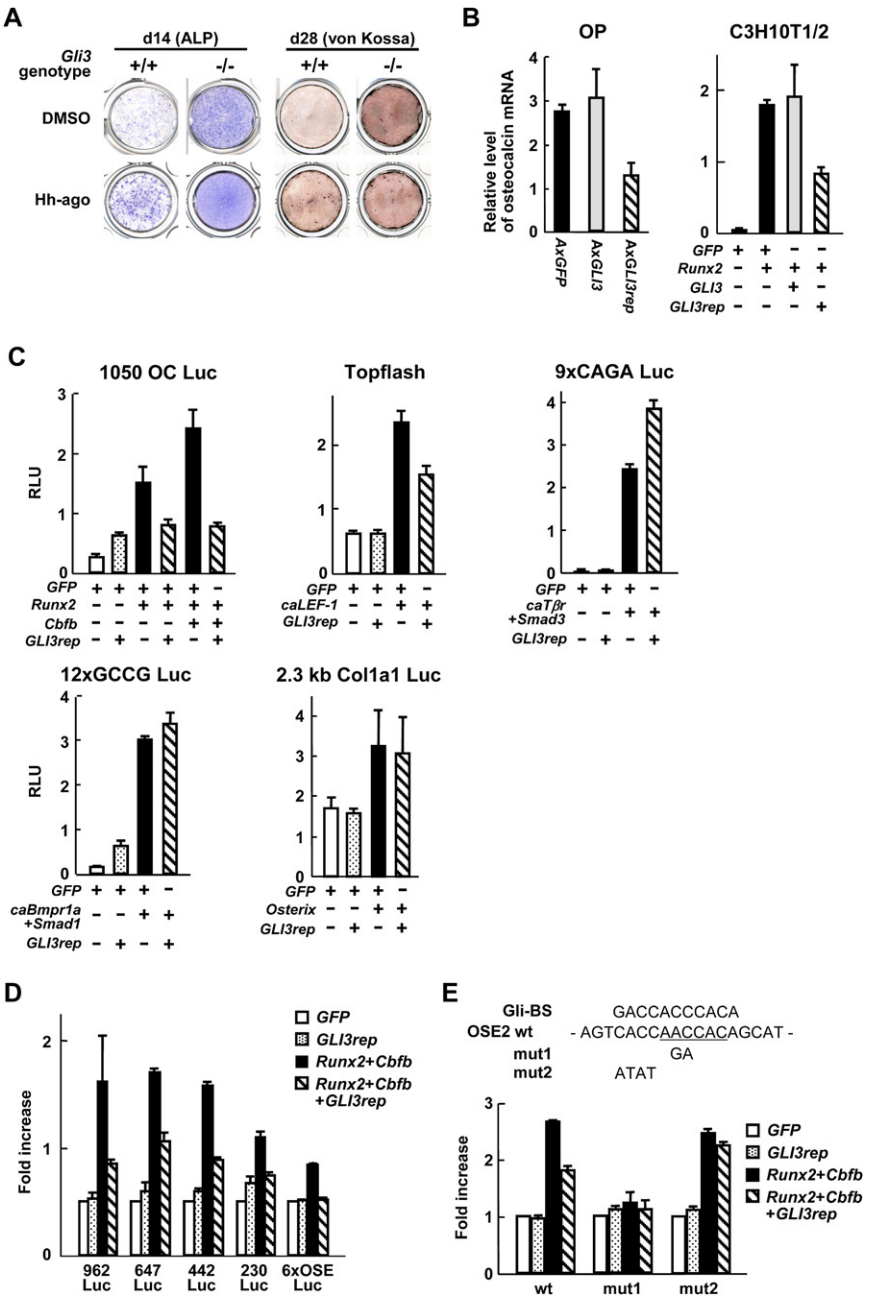

Figure 4. Repression of Runx2-Dependent Transcription by Gli3 Repressor Form

(A) ALP and von Kossa stainings in cultures of calvarial cells from WT and *Gli3*$^{-/-}$. For ALP staining, cells were cultured for 14 days in α-MEM/10% FBS with DMSO or Hh agonist (Hh-ago). For von Kossa staining, cells were cultured for 28 days in α-MEM/10% FBS containing dexamethasone, β-glycerophosphate, and ascorbic acid phosphate, with DMSO or Hh-ago. Representative pictures of independent experiments are shown.

(B) *Osteocalcin* mRNA expression determined by real-time RT-PCR analysis in WT OPs and in C3H10T1/2 cells. WT OPs were cultured for 7 days in α-MEM/10% FBS after infection with adenoviruses expressing *GFP*, *GLI3*, and *GLI3*rep. C3H10T1/2 cells were cultured for 2 days in DMEM/10% FBS after transfection with the indicated plasmids.

(C) Effects of GLI3rep on transcriptional activities of Runx2 (1050 Oc Luc), LEF1-β-catenin (Topflash), Smad3 (9×CAGA Luc), Smad1 (12×GCCG Luc), and Osterix (2.3 kb Col1a1 Luc). NIH 3T3 cells (1050 Oc, Topflash, 9×CAGA, and 12×GCCG Luc) or C3H10T1/2 cells (2.3 kb Col1a1 Luc) were transfected with each reporter plasmid, in combination with the indicated plasmids, and a luciferase assay was performed 48 hr after transfection. caLEF-1, constitutively active lymphoid enhancer factor-1; ca*Tβr*, constitutively active transforming growth factor-β receptor type I; ca*Bmpr1a*, constitutively active BMP receptor type IA.

(D) Transcriptional activity repressed by GLI3rep in deletion mutants of the osteocalcin promoter. Deletion mutants of the osteocalcin promoter of the indicated lengths (962, 647, 442, and 230 bp) were constructed from the 1050 Oc Luc. NIH 3T3 cells were transfected with each mutant reporter plasmid or 6×OSE Luc, in combination with the indicated plasmids.

(E) The effect of mutation in OSE2 on GLI3rep-mediated repression of Runx2-dependent transcriptional activation. The indicated mutation was created in the Runx2-binding site or putative Gli-binding site of the 230 Oc Luc. NIH 3T3 cells were transfected with each reporter plasmid, in combination with the indicated plasmids. For (B)–(E), data are means ± SDs of triplicate wells, and representative data of independent experiments are shown.

osteoblast differentiation by *Ptch1* haploinsufficiency is at least partly attributable to the reduction of this attenuation.

Systemic Interference with Hh Signaling Decreases Bone Mass in Adult Mice

The data so far reveal that the activation of Hh signaling by *Ptch1* haploinsufficiency causes an increase in adult bone mass, raising the possibility that blocking Hh signaling may have a negative impact on adult bone mass. To evaluate this effect, we systemically treated WT mice (8 weeks of age) with cyclopamine, a Hh signaling blocker, and analyzed their skeletal system in comparison with the mice treated with tomatidine, a steroidal alkaloid similar to cyclopamine but without any effects on Hh signaling. After 1 month of treatment, the cyclopamine-treated mice showed a reduction in mRNA expression of *Ptch1* and *Gli1* in bone, indicating that Hh signaling was inhibited (Figure 6A). Their bone mass and bone mineral density were significantly lower than in the tomatidine-treated group, whereas there was no significant difference in body weight (Figures 6B and 6C). Histological and bone histomorphometric analyses revealed a decrease in bone volume in the cyclopamine-treated group, which was attributed to impaired osteoblast differentiation and function (Figures 6D and 6E). As for bone resorption, the number of TRAP-positive osteoclasts and values of all parameters for bone resorption were decreased in the cyclopamine-treated mice (Figures 6D and 6E). Taken together, these findings

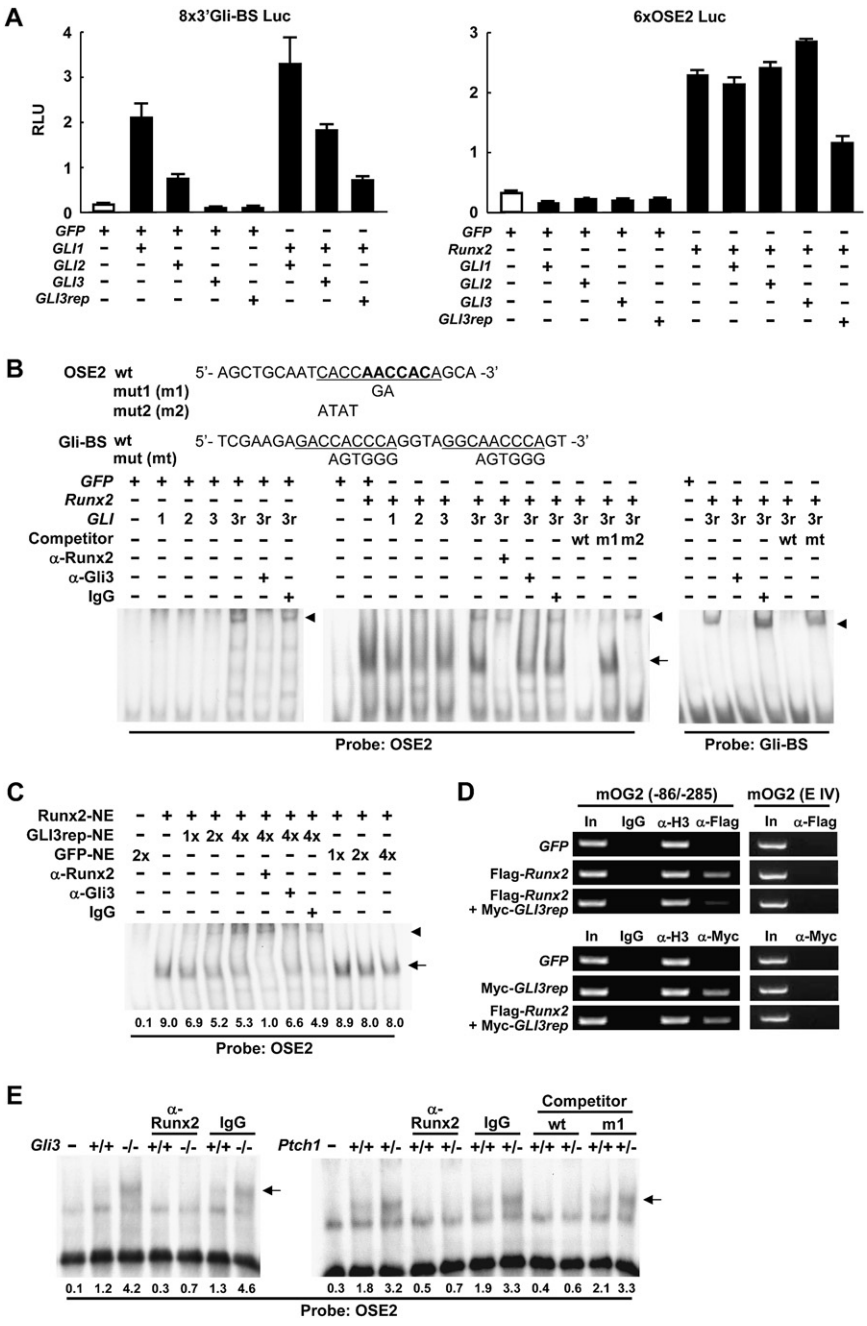

Figure 5. Competitive Inhibition of Runx2 DNA Binding Activity by Gli3 Repressor Form

(A) Comparison of transcriptional activity of the Gli family proteins (Gli1, 2, 3 and 3rep) using 8× Gli-binding site Luc (left, 8×3′Gli-BS Luc) and 6×OSE2 Luc (right). C3H10T1/2 cells were transfected with each reporter plasmid, in combination with the indicated plasmids. Data are means ± SDs of triplicate wells, and representative data of independent experiments are shown.

(B) Binding of Gli3rep to OSE2 determined by EMSA. Oligonucleotide probes containing OSE2 and ones containing the Gli-binding site in human *PTCH1* promoter were used (top). The Runx2-binding sequence is in boldface, and the putative Gli-binding sequence is underlined. Nuclear extracts of COS-7 cells transfected with the indicated plasmids were analyzed using DIG-labeled OSE2 probes (bottom, left) and Gli-BS ones (bottom, right). Arrows, shifted bands of Runx2-DNA complexes; Arrowheads, shifted bands of Gli3rep-DNA complexes.

(C) Inhibitory effect of GLI3rep on DNA binding activity of Runx2. Nuclear extracts of *Runx2*-transfected COS-7 cells were analyzed by EMSA using DIG-labeled OSE2 probes. Increasing amounts (1×, 2×, and 4×) of nuclear extracts of *GLI3rep*-transfected COS-7 cells (*GLI3rep*-NE) or equivalent amounts of those of *GFP*-transfected COS-7 cells (*GFP*-NE) were added to the DNA binding reaction mixture. Arrow, shifted bands of Runx2-DNA complexes. Arrowhead, shifted bands of Gli3rep-DNA complexes.

(D) Recruitment of GLI3rep onto endogenous osteocalcin promoter. ChIP assay was performed on C3H10T1/2 cells cultured for 2 days after transfection with the indicated plasmids. In, PCR from total DNA input for each sample; IgG, PCR from the immunoprecipitation product with normal IgG (negative control); α-H3, PCR from the immunoprecipitation product with anti-acetyl histon H3 (positive control); mOG2 mouse osteocalcin gene 2; E IV, coding region in exon 4.

(E) DNA binding activity of Runx2 in *Gli3*$^{-/-}$ or *Ptch1*$^{+/-}$ OPs. Nuclear extracts of OPs derived from WT and *Gli3*$^{-/-}$ littermates (left) or WT and *Ptch1*$^{+/-}$ ones (right) were analyzed by EMSA using DIG-labeled OSE2 probes. As a negative control, a binding mixture containing COS-7 nuclear extracts and labeled probes was loaded in lane 1. Arrows, shifted bands of Runx2-DNA complexes. For (C) and (E), quantified intensities of shifted bands of Runx2-DNA complexes are shown below each panel.

suggest that systemic interference with Hh signaling causes low-turnover osteopenia in adult mice, showing the importance of Hh-Ptch1 signaling in adult bone homeostasis.

DISCUSSION

The present study had five major findings. First, *Ptch1* haploinsufficiency caused increased bone mass with enhanced osteoblast differentiation. Second, generation of endogenous Gli3rep was repressed in *Ptch1*$^{+/-}$ OPs with the activation of Hh-Ptch1 signaling, and Gli3rep, but not Gli3full, was preferentially localized in the nucleus. Third, Gli3rep attenuated Runx2 transcriptional activity by competitively inhibiting its DNA binding. Fourth, in both *Gli3*$^{-/-}$ and *Ptch1*$^{+/-}$ cells, the DNA-binding activity of Runx2 was augmented. Finally, systemic interference with Hh signaling using an inhibitor resulted in decreased bone mass in adult mice. These findings suggest that Hh-Ptch1 signaling regulates adult bone mass and that this regulation occurs at least partly through modulation of the effect of Gli3rep on osteoblast-related transcription factors.

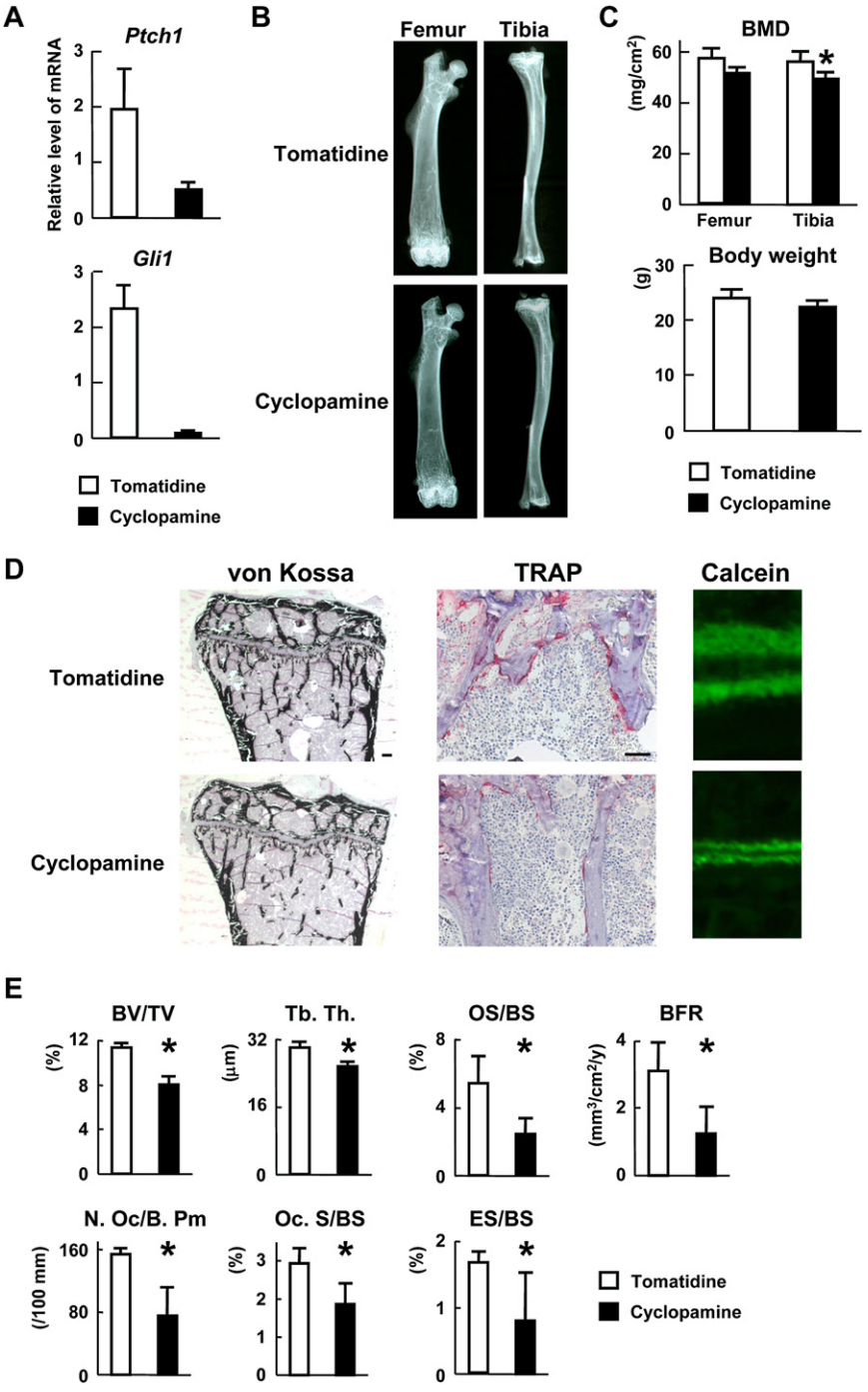

Figure 6. The Effect of Administration of Hh Signaling Inhibitor on Adult Bone Mass

(A) mRNA expression of *Ptch1* and *Gli1* in bone tissue, determined by real-time RT-PCR analysis. Data are means ± SDs of triplicate samples.

(B) Plain X-ray images of the femurs (left) and tibias (right) of representative tomatidine-treated and cyclopamine-treated mice.

(C) Bone mineral density of the whole femurs and tibias (upper) and body weight (lower) of tomatidine-treated and cyclopamine-treated mice. Data are means ± SDs of five mice per treatment. *$p < 0.05$ versus tomatidine-treated mice.

(D) von Kossa staining, TRAP staining, and calcein double labeling of the proximal tibia sections of representative tomatidine-treated and cyclopamine-treated mice. Bar, 300 μm.

(E) Histomorphometric analyses of bone volume and bone formation parameters in the proximal tibia of tomatidine-treated and cyclopamine-treated mice. Data are means ± SDs of five mice per treatment. *$p < 0.05$ versus tomatidine-treated mice.

Bone mass phenotypes in *Ptch1*$^{+/-}$ mice indicate that Hh-Ptch1 signaling has crucial roles not only in forming embryonic bone but also in maintaining adult bone mass. This notion is in harmony with the recent report by Maeda and colleagues that indicates the involvement of Ihh produced by postnatal chondrocytes in sustaining the trabecular bone (Maeda et al., 2007). Moreover, we demonstrate that the direct input of Hh signaling to postnatal skeletal cells affects the bone mass and that Ptch1, a key mediator of various fundamental processes in embryonic development, also controls bone homeostasis in adult tissue. In the accompanying paper, Mak et al. (2008) (in this issue of *Developmental Cell*) report the skeletal phenotype of the mice in which *Ptch1* is disrupted selectively in mature osteoblasts. In common with our findings on conventional mutant mice, both osteoblastogenesis and osteoclastogenesis were enhanced in their mice, suggesting that the activation of Hh-Ptch1 signaling directly induced osteoblastogenesis and indirectly induced osteoclastogenesis via mature osteoblasts. However, their mice showed the opposite phenotypes to ours in terms of bone mass, with bone resorption dominant over bone formation. It is not entirely clear why such a difference arose between their mice and ours, particularly considering the similar changes observed at a cellular level, but a number of factors could be involved. First, the level of modulation of Hh-Ptch1 signaling was different between our study and theirs; ours was a partial modulation (haploinsufficiency mutants and systemic administration of small compounds), while theirs was full (homozygous mutants). It is possible that partial modulation of the Hh-Ptch1 signaling has a dominant impact on bone formation, while full modulation acts dominantly on bone resorption. Second, our mice were conventional mutants in which all the cells were affected from the onset of development, while theirs were conditional ones in which only mature osteoblasts were affected. Thus, their mice may have highlighted a specific role of Hh-Ptch1 signaling in mature osteoblasts' regulation of osteoclastogenesis.

Expression of *Gli1* mRNA was increased in *Ptch1*$^{+/-}$ OPs, indicating constitutive activation of Hh signaling. In contrast, *Ptch1* mRNA was decreased in *Ptch1*$^{+/-}$ OBs. In line with our results, Goodrich and colleagues reported that *Ptch1* mRNA was reduced in *Ptch1*$^{+/-}$ cerebella despite high-level Ptch1 transcription shown by increased expression of *LacZ* fused to Ptch1 alleles (Goodrich et al., 1997). In a physiological context, high-level Ptch1 in response to Hh has been known to limit the effects of Hh signaling by intracellularly attenuating its continuous activation or by preventing its transmission across the cells (Goodrich et al., 1997). Taking these findings together, we speculate that enhanced transcription of *Ptch1* by Hh signaling activation cannot overcome the lack of one copy of the *Ptch1* gene, because the negative feedback loop collapses. As a result, low-level Ptch1 may further accelerate the constitutive activation of Hh signaling in *Ptch1*$^{+/-}$ cells.

We focused on Gli3 as a key downstream mediator of Hh-Ptch1 signaling in osteoblast differentiation for the following reasons. First, as mentioned in the Introduction, a number of reports indicate that Gli3 mainly acts as a transcriptional repressor and that this repressor function regulated by the Hh input has a crucial role in limb development. Second, *Ihh*$^{-/-}$ developing limbs showed higher *Gli3* expression than WT (Hilton et al., 2005). Third, as a consequence of Hh-Ptch1 signaling activation, *Gli3* expression and Gli3rep generation were remarkably repressed in *Ptch1*$^{+/-}$ OPs. Fourth, *Gli3*$^{-/-}$ calvarial cells spontaneously differentiated into osteoblasts and barely responded to a Hh agonist. Although Gli3full was reported to have an activator function in some contexts, Gli3full was preferentially localized in the cytoplasm of OPs. Furthermore, overexpressed Gli3full that had accumulated in the nucleus had no effect on the transcription of osteocalcin mRNA. These findings suggest that Gli3full does not have a major role in the transcription of osteogenesis-related genes.

The role of Gli2 in skeletal development and the positive effect on osteoblast differentiation documented by other researchers (Miao et al., 2004; Mo et al., 1997; Shimoyama et al., 2007; Zhao et al., 2006) raise the possibility that Gli2 might play a role in the effect of *Ptch1* haploinsufficiency on osteoblast differentiation. However, we think it unlikely that Gli2 is a main mediator, at least in *Ptch1* haploinsufficiency, because no alteration of Gli2 expression, localization, or processing was observed between *Ptch1*$^{+/-}$ and WT OPs. Supporting our findings, the expression level of *Gli2* in the *Ihh*$^{-/-}$ perichondrium was reported to be comparable to that in WT (Hilton et al., 2005). On the other hand, our findings seem inconsistent with reports that overexpressed Gli2 in C3H10T1/2 cells translocated into the nucleus upon Ihh treatment (Shimoyama et al., 2007) or with reports that Shh treatment of fibroblasts suppressed endogenous Gli2 processing and degradation (Pan et al., 2006). Our findings also may not concur with the reports that Gli2 induced *Bmp2* expression and that Gli3rep repressed the expression (Garrett et al., 2003; Zhao et al., 2006), while we showed that endogenous *Bmp2* expression was not markedly upregulated in *Ptch1*$^{+/-}$. Discrepancies between our findings and others described so far may arise from differences of cell types (primary cells versus cell lines; osteoblasts versus fibroblasts). Alternatively, *Ptch1* haploinsufficiency may lead to less activation of Hh signaling or less alteration of Gli expression than treatment with Hh proteins or overexpresion of Gli. It remains to be determined whether Hh-Ptch1 signaling induces osteoblast differentiation through Gli2. Analysis of the effect of Hh treatment on Bmp2 expression, Runx2 function, and osteoblast differentiation in *Gli2* knockout cells may help address this question.

Regarding BMP and Hh-Ptch1 signaling, we also demonstrated that responsiveness to exogenous BMP2 was increased in *Ptch1*$^{+/-}$ cells compared to WT cells. In line with our results, Hh-Ptch1 signaling has been shown to modify cellular responsiveness to other signals, including several members of the BMP family (Murtaugh et al., 1999). Based on our findings, we infer that, in osteogenesis, Hh-Ptch1 signaling modifies the cellular responsiveness to BMP by regulating Gli3's antagonistic actions against Runx2.

To determine how Gli3rep attenuated the transcriptional activity of Runx2, we considered four potential mechanisms of the attenuation (Latchman, 1996): (1) squelching of the basal transcriptional machinery, (2) prevention of DNA binding of Runx2, (3) quenching of the transactivation properties of DNA-bound Runx2, and (4) recruitment of a corepressor. By EMSA and ChIP, we demonstrated specific binding of Gli3rep to OSE2 and Gli3rep's inhibitory effect on the DNA binding of Runx2. In addition, physical interaction between Runx2 and Gli3rep was not discernable. Based on these results, we propose that Gli3rep represses Runx2 by competitively preventing its DNA binding. Squelching does not appear to be the mechanism, because Gli3rep failed to repress the basal activity of Oc-luc. On the other hand, Gli3rep was reported to interact with the histone deacetylase 1 (HDAC1) and the Ski corepressor (Dai et al., 2002), raising the possibility that Gli3rep may regulate transcription by reversing chromatin remodeling and/or recruiting corepressors. Although further work is needed, we suggest that this may not be the main mechanism of Runx2 attenuation by Gli3rep because we observed strong attenuation of Runx2-induced transcription by Gli3rep in the luciferase assays, in which exogenous plasmids typically do not assume the normal chromatin structure, and there was no marked alteration in histone H3 acetylation by ChIP.

Our findings may not concur with a recent report by Shimoyama and colleagues in which in vitro data indicated that overexpressed Gli2 enhanced Runx2 function through physical interaction (Shimoyama et al., 2007). The discrepancy may arise from the difference in the structures of reporter constructs. However, the physiological role of Gli2 in *Ptch1*$^{+/-}$ seems unclear, because no alteration of Gli2 expression, localization, or processing was observed between *Ptch1*$^{+/-}$ and WT OPs.

In conclusion, we have identified Hh-Ptch1 signaling as a crucial regulator of postnatal bone homeostasis. Alteration of Hh-Ptch1 signaling due to genetic anomaly or drugs may affect bone mass in patients at any age. Based on our study and that of Mak et al. (2008), it is clear that Hh-Ptch1 signaling can be a potential molecular target for the treatment of osteoporosis. At the same time, in the modulation of Hh-Ptch1 signaling, it is necessary to consider the level of the modulation, as well as the target cells and timing, because those factors may significantly influence the outcome.

EXPERIMENTAL PROCEDURES

Animal Experiments

Ptch1^{tm1Mps} (*Ptch*$^{+/-}$) and *Gli3*$^{Xt\text{-}J}$ (*Gli3*$^{+/-}$) mice were obtained from Jackson Laboratory (Bar Harbor, ME); wild-type C57BL/6N mice were obtained from

Charles River Japan (Kanagawa, Japan). Histological, histomorphometric, and radiological analyses were performed as described (Kugimiya et al., 2005). NIH Image was used to measure the ratio of the trabecular bone area to the total area. In cyclopamine treatment of mice, cyclopamine and tomatidine (BIOMOL International, Plymouth Meeting, PA) were dissolved in a solution of 45% of 2-hydroxypropyl-b-cyclodextrin (HBC, Sigma-Aldrich) in PBS at 1 mg/ml, as described (Sanchez and Ruiz i Altaba, 2005). Mice received intraperitoneal injections of either 10 mg/kg of HBC-cyclopamine or HBC-tomatidine beginning at 8 weeks of age and every day thereafter for a month. All experiments were performed on male mice in accordance with the protocol approved by the Animal Care and Use Committee of the University of Tokyo.

Cell Culture

NIH 3T3, COS-7, and C3H10T1/2 cells were obtained from the RIKEN Cell Bank (Tsukuba, Japan). Isolation of bone marrow stromal cells from long bones or of osteoblast precursors from calvaria, osteogenic culture (Ogata et al., 2000; Akune et al., 2004), in vitro osteoclast formation from BMMϕs (Katagiri et al., 2006) or RAW264.7 cells (Ogasawara et al., 2004a), and the coculture of OPs and BMMϕ (Akune et al., 2004; Ogata et al., 2000) were performed as described. Cell proliferation was quantified using a Cell Counting Kit-8 (Wako Pure Chemical Industry, Osaka, Japan). Recombinant human (rh) BMP2 and Hh agonist (Cur-0199567; Frank-Kamenetsky et al., 2002) were used at 200 ng/ml and 10 nM, respectively. Plasmid transfection was performed using FuGENE6 (Roche, Penzberg, Germany); adenoviruses were infected at 50 MOI (multiplicity of infection). Alkaline phosphatase (ALP) and von Kossa stainings were performed as described (Kugimiya et al., 2005).

Real-Time RT-PCR

Total RNA extraction, reverse-transcription, and real-time PCR were performed as described (Kugimiya et al., 2005). All reactions were run in triplicate. The primer sequences are available upon request.

Luciferase Assay

Cells were plated onto 24-well plates and transfected with 0.4 μg of DNA mixture containing the test reporter plasmids, the control reporter plasmids encoding *Renilla* luciferase, and the effector plasmids. The dual luciferase assay was performed 48 hr after transfection as described (Yano et al., 2005).

Immunoblot and Coimmunoprecipitation

Whole-cell lysates were isolated using RIPA buffer as described (Ogasawara et al., 2004b). Separated extraction of cytoplasmic and nuclear proteins was performed using the NE-PER Kit (Pierce Chemical, Rockford, IL). SDS-PAGE and immunoblotting were performed as described (Yano et al., 2005). Band intensities were calculated using Quantity One (Bio-Rad Laboratories, Hercules, CA). Coimmunoprecipitation was performed using the Catch and Release Kit (Upstate, Lake Placid, NY) and 2 μg of specific antibodies.

ChIP

ChIP was performed using EZ ChIP (Upstate). PCR was performed to amplify the promoter region (−86/−285) and the coding region (exon 4) of the mouse osteocalcin.

EMSA

Nuclear extracts were obtained as described (Dignam et al., 1983). hGLI3rep protein was translated in vitro using TNT Quick Coupled Transcription/Translation Systems (Promega, Madison, WI) and pCITE-4a vectors (Novagen, Darmstadt, Germany). Digoxigenin (DIG)-labeled probes were constructed using the DIG Gel Shift Kit (Roche).

Statistical Analysis

The means of groups were compared by ANOVA, and the significance of differences was determined by post hoc testing using Bonferroni's method.

SUPPLEMENTAL DATA

Supplemental data include eight figures, one table, Supplemental Experimental Procedures, and Supplemental References and are available at http://www.developmentalcell.com/cgi/content/full/14/5/689/DC1/.

ACKNOWLEDGMENTS

We thank K. Miyazono, T. Komori, G. Karsenty, G.S. Stein, A. Hecht, T. Katagiri, R. Nishimura, A. Ruiz i Altaba, J.Y. Choi, and H. Sasaki for their kind provision of experimental materials. We also appreciate the helpful discussions with members of the Chung lab and the Department of Orthopaedic Surgery, University of Tokyo; R. Yamaguchi, K. Morii, Y. Hasegawa, M. Zenibayashi, K. Suzuki, H. Murayama, and the hard-tissue research team at Kureha Chemical Industry Co. for providing technical assistance; Astellas Pharma Inc. for providing rhBMP2; and Curis Inc. for providing Hh agonist. This work was supported by Grants-in-Aid for Scientific Research from the Japanese Ministry of Education, Culture, Sports, Science, and Technology (#18659437 and #17390530).

Received: September 13, 2007
Revised: January 13, 2008
Accepted: March 12, 2008
Published: May 12, 2008

REFERENCES

Akune, T., Ohba, S., Kamekura, S., Yamaguchi, M., Chung, U.I., Kubota, N., Terauchi, Y., Harada, Y., Azuma, Y., Nakamura, K., et al. (2004). PPARgamma insufficiency enhances osteogenesis through osteoblast formation from bone marrow progenitors. J. Clin. Invest. *113*, 846–855.

Bae, J.S., Gutierrez, S., Narla, R., Pratap, J., Devados, R., van Wijnen, A.J., Stein, J.L., Stein, G.S., Lian, J.B., and Javed, A. (2007). Reconstitution of Runx2/Cbfa1-null cells identifies a requirement for BMP2 signaling through a Runx2 functional domain during osteoblast differentiation. J. Cell. Biochem. *100*, 434–449.

Chung, U.I., Schipani, E., McMahon, A.P., and Kronenberg, H.M. (2001). Indian hedgehog couples chondrogenesis to osteogenesis in endochondral bone development. J. Clin. Invest. *107*, 295–304.

Dai, P., Shinagawa, T., Nomura, T., Harada, J., Kaul, S.C., Wadhwa, R., Khan, M.M., Akimaru, H., Sasaki, H., Colmenares, C., et al. (2002). Ski is involved in transcriptional regulation by the repressor and full-length forms of Gli3. Genes Dev. *16*, 2843–2848.

Dignam, J.D., Lebovitz, R.M., and Roeder, R.G. (1983). Accurate transcription initiation by RNA polymerase II in a soluble extract from isolated mammalian nuclei. Nucleic Acids Res. *11*, 1475–1489.

Ducy, P., Zhang, R., Geoffroy, V., Ridall, A.L., and Karsenty, G. (1997). Osf2/Cbfa1: a transcriptional activator of osteoblast differentiation. Cell *89*, 747–754.

Frank-Kamenetsky, M., Zhang, X.M., Bottega, S., Guicherit, O., Wichterle, H., Dudek, H., Bumcrot, D., Wang, F.Y., Jones, S., Shulok, J., et al. (2002). Small-molecule modulators of Hedgehog signaling: identification and characterization of Smoothened agonists and antagonists. J. Biol. *1*, 10.

Fujii, K., Kohno, Y., Sugita, K., Nakamura, M., Moroi, Y., Urabe, K., Furue, M., Yamada, M., and Miyashita, T. (2003a). Mutations in the human homologue of Drosophila patched in Japanese nevoid basal cell carcinoma syndrome patients. Hum. Mutat. *21*, 451–452.

Fujii, K., Miyashita, T., Omata, T., Kobayashi, K., Takanashi, J., Kouchi, K., Yamada, M., and Kohno, Y. (2003b). Gorlin syndrome with ulcerative colitis in a Japanese girl. Am. J. Med. Genet. A. *121*, 65–68.

Garrett, I.R., Chen, D., Gutierrez, G., Zhao, M., Escobedo, A., Rossini, G., Harris, S.E., Gallwitz, W., Kim, K.B., Hu, S., et al. (2003). Selective inhibitors of the osteoblast proteasome stimulate bone formation in vivo and in vitro. J. Clin. Invest. *111*, 1771–1782.

Goodrich, L.V., Milenkovic, L., Higgins, K.M., and Scott, M.P. (1997). Altered neural cell fates and medulloblastoma in mouse patched mutants. Science *277*, 1109–1113.

Gorlin, R.J. (1987). Nevoid basal-cell carcinoma syndrome. Medicine (Baltimore) *66*, 98–113.

Hilton, M.J., Tu, X., Cook, J., Hu, H., and Long, F. (2005). Ihh controls cartilage development by antagonizing Gli3, but requires additional effectors to regulate osteoblast and vascular development. Development *132*, 4339–4351.

Hoffmann, A., and Gross, G. (2001). BMP signaling pathways in cartilage and bone formation. Crit. Rev. Eukaryot. Gene Expr. *11*, 23–45.

Hui, C.C., and Joyner, A.L. (1993). A mouse model of greig cephalopolysyndactyly syndrome: the extra-toesJ mutation contains an intragenic deletion of the Gli3 gene. Nat. Genet. *3*, 241–246.

Ingham, P.W., and McMahon, A.P. (2001). Hedgehog signaling in animal development: paradigms and principles. Genes Dev. *15*, 3059–3087.

Johnston, J.J., Olivos-Glander, I., Killoran, C., Elson, E., Turner, J.T., Peters, K.F., Abbott, M.H., Aughton, D.J., Aylsworth, A.S., Bamshad, M.J., et al. (2005). Molecular and clinical analyses of Greig cephalopolysyndactyly and Pallister-Hall syndromes: robust phenotype prediction from the type and position of GLI3 mutations. Am. J. Hum. Genet. *76*, 609–622.

Katagiri, M., Ogasawara, T., Hoshi, K., Chikazu, D., Kimoto, A., Noguchi, M., Sasamata, M., Harada, S., Akama, H., Tazaki, H., et al. (2006). Suppression of adjuvant-induced arthritic bone destruction by cyclooxygenase-2 selective agents with and without inhibitory potency against carbonic anhydrase II. J. Bone Miner. Res. *21*, 219–227.

Komori, T., Yagi, H., Nomura, S., Yamaguchi, A., Sasaki, K., Deguchi, K., Shimizu, Y., Bronson, R.T., Gao, Y.H., Inada, M., et al. (1997). Targeted disruption of Cbfa1 results in a complete lack of bone formation owing to maturational arrest of osteoblasts. Cell *89*, 755–764.

Kugimiya, F., Kawaguchi, H., Kamekura, S., Chikuda, H., Ohba, S., Yano, F., Ogata, N., Katagiri, T., Harada, Y., Azuma, Y., et al. (2005). Involvement of endogenous bone morphogenetic protein (BMP) 2 and BMP6 in bone formation. J. Biol. Chem. *280*, 35704–35712.

Latchman, D.S. (1996). Inhibitory transcription factors. Int. J. Biochem. Cell Biol. *28*, 965–974.

Litingtung, Y., Dahn, R.D., Li, Y., Fallon, J.F., and Chiang, C. (2002). Shh and Gli3 are dispensable for limb skeleton formation but regulate digit number and identity. Nature *418*, 979–983.

Liu, F., Massague, J., and Ruiz i Altaba, A. (1998). Carboxy-terminally truncated Gli3 proteins associate with Smads. Nat. Genet. *20*, 325–326.

Long, F., Chung, U.I., Ohba, S., McMahon, J., Kronenberg, H.M., and McMahon, A.P. (2004). Ihh signaling is directly required for the osteoblast lineage in the endochondral skeleton. Development *131*, 1309–1318.

Mak, K.K., Bi, Y., Wan, C., Chuang, P.-T., Clemens, T., Young, M., and Yang, Y. (2008). Hedgehog signaling in mature osteoblasts regulates bone formation and resorption by controlling PTHrP and RANKL expression. Dev. Cell *14*, this issue, 674–688.

Maeda, Y., Nakamura, E., Nguyen, M.T., Suva, L.J., Swain, F.L., Razzaque, M.S., Mackem, S., and Lanske, B. (2007). Indian Hedgehog produced by postnatal chondrocytes is essential for maintaining a growth plate and trabecular bone. Proc. Natl. Acad. Sci. USA *104*, 6382–6387.

Miao, D., Liu, H., Plut, P., Niu, M., Huo, R., Goltzman, D., and Henderson, J.E. (2004). Impaired endochondral bone development and osteopenia in Gli2-deficient mice. Exp. Cell Res. *294*, 210–222.

Milenkovic, L., Goodrich, L.V., Higgins, K.M., and Scott, M.P. (1999). Mouse patched1 controls body size determination and limb patterning. Development *126*, 4431–4440.

Mo, R., Freer, A.M., Zinyk, D.L., Crackower, M.A., Michaud, J., Heng, H.H., Chik, K.W., Shi, X.M., Tsui, L.C., Cheng, S.H., et al. (1997). Specific and redundant functions of Gli2 and Gli3 zinc finger genes in skeletal patterning and development. Development *124*, 113–123.

Murtaugh, L.C., Chyung, J.H., and Lassar, A.B. (1999). Sonic hedgehog promotes somitic chondrogenesis by altering the cellular response to BMP signaling. Genes Dev. *13*, 225–237.

Ogasawara, T., Katagiri, M., Yamamoto, A., Hoshi, K., Takato, T., Nakamura, K., Tanaka, S., Okayama, H., and Kawaguchi, H. (2004a). Osteoclast differentiation by RANKL requires NF-kappaB-mediated downregulation of cyclin-dependent kinase 6 (Cdk6). J. Bone Miner. Res. *19*, 1128–1136.

Ogasawara, T., Kawaguchi, H., Jinno, S., Hoshi, K., Itaka, K., Takato, T., Nakamura, K., and Okayama, H. (2004b). Bone morphogenetic protein 2-induced osteoblast differentiation requires Smad-mediated down-regulation of Cdk6. Mol. Cell. Biol. *24*, 6560–6568.

Ogata, N., Chikazu, D., Kubota, N., Terauchi, Y., Tobe, K., Azuma, Y., Ohta, T., Kadowaki, T., Nakamura, K., and Kawaguchi, H. (2000). Insulin receptor substrate-1 in osteoblast is indispensable for maintaining bone turnover. J. Clin. Invest. *105*, 935–943.

Ohba, S., Ikeda, T., Kugimiya, F., Yano, F., Lichtler, A.C., Nakamura, K., Takato, T., Kawaguchi, H., and Chung, U.I. (2007). Identification of a potent combination of osteogenic genes for bone regeneration using embryonic stem (ES) cell-based sensor. FASEB J. *21*, 1777–1787.

Pan, Y., Bai, C.B., Joyner, A.L., and Wang, B. (2006). Sonic hedgehog signaling regulates Gli2 transcriptional activity by suppressing its processing and degradation. Mol. Cell. Biol. *26*, 3365–3377.

Park, H.L., Bai, C., Platt, K.A., Matise, M.P., Beeghly, A., Hui, C.C., Nakashima, M., and Joyner, A.L. (2000). Mouse Gli1 mutants are viable but have defects in SHH signaling in combination with a Gli2 mutation. Development *127*, 1593–1605.

Phimphilai, M., Zhao, Z., Boules, H., Roca, H., and Franceschi, R.T. (2006). BMP signaling is required for RUNX2-dependent induction of the osteoblast phenotype. J. Bone Miner. Res. *21*, 637–646.

Sanchez, P., and Ruiz i Altaba, A. (2005). In vivo inhibition of endogenous brain tumors through systemic interference of Hedgehog signaling in mice. Mech. Dev. *122*, 223–230.

Sasaki, H., Nishizaki, Y., Hui, C., Nakafuku, M., and Kondoh, H. (1999). Regulation of Gli2 and Gli3 activities by an amino-terminal repression domain: implication of Gli2 and Gli3 as primary mediators of Shh signaling. Development *126*, 3915–3924.

Shimoyama, A., Wada, M., Ikeda, F., Hata, K., Matsubara, T., Nifuji, A., Noda, M., Amano, K., Yamaguchi, A., Nishimura, R., et al. (2007). Ihh/Gli2 signaling promotes osteoblast differentiation by regulating Runx2 expression and function. Mol. Biol. Cell *18*, 2411–2418.

St-Jacques, B., Hammerschmidt, M., and McMahon, A.P. (1999). Indian hedgehog signaling regulates proliferation and differentiation of chondrocytes and is essential for bone formation. Genes Dev. *13*, 2072–2086.

Ulloa, F., Itasaki, N., and Briscoe, J. (2007). Inhibitory Gli3 activity negatively regulates Wnt/beta-catenin signaling. Curr. Biol. *17*, 545–550.

Wang, B., Fallon, J.F., and Beachy, P.A. (2000). Hedgehog-regulated processing of Gli3 produces an anterior/posterior repressor gradient in the developing vertebrate limb. Cell *100*, 423–434.

Wetmore, C., Eberhart, D.E., and Curran, T. (2000). The normal patched allele is expressed in medulloblastomas from mice with heterozygous germ-line mutation of patched. Cancer Res. *60*, 2239–2246.

Yang, S., Wei, D., Wang, D., Phimphilai, M., Krebsbach, P.H., and Franceschi, R.T. (2003). In vitro and in vivo synergistic interactions between the Runx2/Cbfa1 transcription factor and bone morphogenetic protein-2 in stimulating osteoblast differentiation. J. Bone Miner. Res. *18*, 705–715.

Yano, F., Kugimiya, F., Ohba, S., Ikeda, T., Chikuda, H., Ogasawara, T., Ogata, N., Takato, T., Nakamura, K., Kawaguchi, H., et al. (2005). The canonical Wnt signaling pathway promotes chondrocyte differentiation in a Sox9-dependent manner. Biochem. Biophys. Res. Commun. *333*, 1300–1308.

Zhao, M., Qiao, M., Harris, S.E., Chen, D., Oyajobi, B.O., and Mundy, G.R. (2006). The zinc finger transcription factor Gli2 mediates bone morphogenetic protein 2 expression in osteoblasts in response to hedgehog signaling. Mol. Cell. Biol. *26*, 6197–6208.